

Available online at [www.sciencedirect.com](http://www.sciencedirect.com)

ScienceDirect

[www.elsevier.com/locate/jes](http://www.elsevier.com/locate/jes)

**JES**  
 JOURNAL OF  
 ENVIRONMENTAL  
 SCIENCES  
[www.jesc.ac.cn](http://www.jesc.ac.cn)

Q1 **Nanoencapsulation of hexavalent chromium with**  
 2 **nanoscale zero-valent iron: High resolution**  
 3 **chemical mapping of the passivation layer**

Q3 Q2 **Xiao-yue Huang, Lan Ling, Wei-xian Zhang\***

5 State Key Laboratory for Pollution Control, College of Environmental Science and Engineering, Tongji University, Shanghai 200092, China.

Q4 E-mail: [1210411@tongji.edu.cn](mailto:1210411@tongji.edu.cn)

7

9 0 A R T I C L E I N F O

16 Article history:

12 Received 26 November 2017

18 Revised 24 January 2018

19 Accepted 25 January 2018

26 Available online xxxx

21 Keywords:

22 Nanoscale zero-valent iron (nZVI)

23 Hexavalent chromium

24 Solid phase reaction

25 Passivation

26 Spherical-aberration-corrected

27 scanning transmission electron

28 microscopy (Cs-STEM)

29

31

32

33

34

35

36

A B S T R A C T

Solid phase reactions of Cr(VI) with Fe(0) were investigated with spherical-aberration-corrected scanning transmission electron microscopy (Cs-STEM) integrated with X-ray energy-dispersive spectroscopy (XEDS). Near-atomic resolution elemental mappings of Cr(VI)–Fe(0) reactions were acquired. Experimental results show that rate and extent of Cr(VI) encapsulation are strongly dependent on the initial concentration of Cr(VI) in solution. Low Cr loading in nZVI (<1.0 wt%) promotes the electrochemical oxidation and continuous corrosion of nZVI while high Cr loading (>1.0 wt%) can quickly shut down the Cr uptake. With the progress of iron oxidation and dissolution, elements of Cr and O counter-diffuse into the nanoparticles and accumulate in the core region at low levels of Cr(VI) (e.g., <10 mg/L). Whereas the reacted nZVI is quickly coated with a newly-formed layer of 2–4 nm in the presence of concentrated Cr(VI) (e.g., >100 mg/L). The passivation structure is stable over a wide range of pH except when pH is low enough to dissolve the passivation layer. X-ray photoelectron spectroscopy (XPS) depth profiling reconfirms that the composition of the newly-formed surface layer consists of Fe(III)–Cr(III) (oxy)hydroxides with Cr(VI) adsorbed on the outside surface. The insoluble and insulating Fe(III)–Cr(III) (oxy)hydroxide layer can completely cover the nZVI surface above the critical Cr loading and shield the electron transfer. Thus, the fast passivation of nZVI in high Cr(VI) solution is detrimental to the performance of nZVI for Cr(VI) treatment and remediation.

© 2018 The Research Center for Eco-Environmental Sciences, Chinese Academy of Sciences.

Published by Elsevier B.V.

39 Introduction

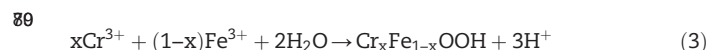
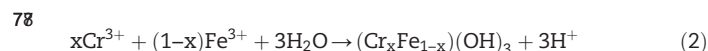
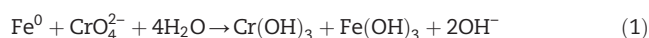
51 Chromium has found numerous industrial applications, such as  
 52 leather tanning, corrosion prevention, mineral extraction, ore  
 53 refining and metal electroplating. Due to improper disposal and  
 54 inefficient treatment, large amounts of chromium-containing  
 55 wastewater and chromium residues have been released to  
 56 the environment. As a result, detections of elevated levels of  
 57 chromium in surface and ground waters, sediments and soils

58 have been wide spread (Cao et al., 2010; Dhal et al., 2013; Gao and  
 59 Xia, 2011; Saha et al., 2011; Wang et al., 2012; Yu et al., 2008).

60 Chromium compounds, especially Cr(VI) species, are highly  
 61 toxic, nonbiodegradable, and bioaccumulative, subsequently  
 62 they tend to persist in the environment and present a long-  
 63 lasting threat to the environment and human health (Bagchi  
 64 et al., 2002; Cervantes et al., 2001; Pellerin and Booker, 2000;  
 65 Salnikow and Zhitkovich, 2007). Reduction of Cr(VI) to less soluble  
 66 Cr(III) species can reduce toxicity, mobility, and availability to

\* Corresponding author. E-mail: [zhangwx@tongji.edu.cn](mailto:zhangwx@tongji.edu.cn) (Wei-xian Zhang).

67 biota, thus providing a mechanism for chromium stabilization  
68 and remediation (Chen et al., 2007; Ellis et al., 2002; Shanker et al.,  
69 2005). For example, zero-valent iron [Fe(0)] has been demon-  
70 strated as an excellent reductant for Cr(VI) treatment (Blowes  
71 et al., 1997; Cundy et al., 2008; Fu et al., 2014, 2013; Ponder et al.,  
72 2000; Wilkin et al., 2005). The Cr(VI) removal by Fe(0) involves  
73 reduction of dissolved Cr(VI) to Cr(III) and the subsequent  
74 precipitation of insoluble Cr(OH)<sub>3</sub> and Fe(III)-Cr(III) (oxy)hydrox-  
75 ides (Cao and Zhang, 2006; Manning et al., 2007; Powell et al.,  
76 1995):



83 Among numerous forms and sizes of Fe(0), the performances  
84 of nanoscale zero-valent iron (nZVI) and its derivatives have  
85 received significant attentions (Adeleye et al., 2016; Ai et al.,  
86 2008; Bhunia et al., 2012; Li et al., 2008; Rajajayavel and Ghoshal,  
87 2015; Shi et al., 2011; Su et al., 2014; WooáLee and BináKim, 2011;  
88 Xia et al., 2017; Xu and Zhao, 2007; Yirsaw et al., 2016). nZVI  
89 has shown higher reduction rate and much higher removal  
90 capacity due to its diminutive size, large specific surface area,  
91 and high surface activity. For example, studies observed that  
92 under similar conditions, the reduction capacity of nZVI was  
93 50–100 times greater than that of micro-scale ZVI, and the  
94 reaction rate with the nZVI was at least 25–30 times faster  
95 (Alowitz and Scherer, 2002; Cao and Zhang, 2006; Li et al., 2008).

96 Most of previous studies have focused on the removal rate  
97 and efficiency of Cr(VI) by nZVI, also the environmental factors  
98 in aqueous solutions as such as pH, dissolved oxygen, Cr(VI)-Fe  
99 (0) ratio, and co-existing substances (Lai and Lo, 2008; Liu et al.,  
100 2008; Lo et al., 2006; Ye et al., 2017). Relatively much less has  
101 been published on the structural evolution and solid phase  
102 reaction mechanisms, which are fundamental to optimization  
103 of nZVI technology for chromium treatment and remediation.  
104 In particular, the deposition of Cr(OH)<sub>3</sub> and/or Fe(III)-Cr(III) (oxy)  
105 hydroxides on the outer surface of nZVI may have a great  
106 impact on the continuing reactions of Cr(VI) with the underlying  
107 metallic iron. The reduction of Cr(VI) by nZVI is to certain degree  
108 self-inhibiting as the insoluble and insulating Cr(III) deposition  
109 on nZVI surface can act as a physical and chemical barrier  
110 and block the electron transfer from Fe(0) to the solid-liquid  
111 interface, thus impede the further reduction of Cr(VI) (Hu et al.,  
112 2010; Melitas et al., 2001; Melitas and Farrell, 2002). In-depth  
113 study of the surface reaction processes, especially the  
114 intraparticle diffusion and transformation in the solid  
115 phase, has significant value in understanding the Cr(VI)-  
116 nZVI reaction mechanisms and activity change of nZVI.

117 Objectives of this study include: (1) to characterize the fine  
118 structure and composition of nZVI after reacting with Cr(VI); (2) to  
119 identify the nanoscale Fe-Cr passivation layer; (3) to assess the  
120 impact of surface passivation on Cr(VI) removal. Electrochemical  
121 tests were conducted to monitor the corrosion/passivation  
122 behavior of reacted nZVI. A state-of-the-art spherical-aberration-  
123 corrected scanning transmission electron microscopy (Cs-STEM)  
124 integrated with X-ray energy-dispersive spectroscopy (XEDS) was  
125 applied to map the reactions of Cr(VI), and to gain near atomic-  
126 scale details on the elemental distribution and translocations

of Fe, O and Cr within a single nanoparticle. Recent advance in  
127 Cs-STEM enables the direct visualization of the pollutant-nZVI  
128 reactions with high spatial resolution and chemical sensitivity  
129 (Huang et al., 2017; Ling et al., 2015; Ling and Zhang, 2015, 2017).  
130 Furthermore, high-resolution X-ray photoelectron spectroscopy  
131 (HR-XPS) combined with Ar<sup>+</sup> sputtering for depth profiling was  
132 utilized to investigate the variations of elemental distribution  
133 and chemical states. 134

## 1. Materials and methods 136

### 1.1. Chemicals and materials 137

All reagents used (e.g., FeCl<sub>3</sub>·6H<sub>2</sub>O, NaBH<sub>4</sub>, and K<sub>2</sub>Cr<sub>2</sub>O<sub>7</sub>) were  
138 analytical-grade or better. The nickel foam (thickness: 1.2 mm,  
139 pore density: 110 PPI) was supplied by Kunshan Jiayisheng  
140 Electronics Co. Ltd. (Jiangsu, China). Fresh nZVI was prepared  
141 by the reduction of ferric chloride with sodium borohydride  
142 following the procedures published previously (Glavee et al.,  
143 1995; Li and Zhang, 2006; Wang and Zhang, 1997). 144

### 1.2. Batch experiments 145

Batch experiments were conducted in 50 mL serum bottles, with  
146 1 g/L nZVI or micro-scale zero-valent iron (mZVI, 400 mesh)  
147 added to 35 mL of 10–1000 mg/L Cr(VI) solution. The batch  
148 bottles were sealed with screw caps and mixed on a shaker  
149 table (180 r/min) at ambient temperature. To eliminate the  
150 potential effect of dissolved oxygen (DO), the Cr(VI) solutions  
151 were purged with high-purity nitrogen (>99.9%) for 30 min prior  
152 to the introduction of iron. Solution pH was adjusted to desired  
153 values by adding dilute solution of NaOH or HCl at the start  
154 of experiments. After 24 hr, the samples were withdrawn and  
155 then filtrated with 0.22 μm PTFE syringe filters prior to analysis.  
156 The residual Cr concentrations in the filtrate were determined  
157 using inductively coupled plasma spectrometers (ICP-OES,  
158 Agilent 720ES and ICP-MS, Agilent 7700). 159

### 1.3. Electrochemical measurements 160

Electrochemical measurements were performed with a CHI660A  
161 electrochemical workstation (Shanghai Chenhua Co. Ltd., China).  
162 A traditional three-electrode cell was used. The reference  
163 electrode was a saturated calomel electrode (SCE) and the counter  
164 electrode was made of a platinum foil (1.0 cm × 1.5 cm). Iron  
165 nanoparticle arrays supported on nickel foam were prepared to  
166 act as the working electrode. Details about fabrication of the  
167 working electrode can be found in the Electronic Supplementary  
168 Material. The polarization tests in 10 mmol/L NaCl background  
169 electrolyte solution were measured by scanning the potential at  
170 1 mV/s from -1.0 to 1.0 V. 171

### 1.4. STEM characterization 172

A FEI Titan™ G2 60-300 spherical-aberration-corrected scan-  
173 ning transmission electron microscopy (Cs-STEM) integrated  
174 with X-ray energy-dispersive spectroscopy (XEDS) was operated  
175 at 200 kV to perform the morphological, structural and elemen-  
176 tal characterization on the Cr(VI) reactions in nZVI. Samples for  
177

Download English Version:

<https://daneshyari.com/en/article/8865465>

Download Persian Version:

<https://daneshyari.com/article/8865465>

[Daneshyari.com](https://daneshyari.com)